COMPDYN 2011
III ECCOMAS Thematic Conference on
Computational Methods in Structural Dynamics and Earthquake Engineering
M. Papadrakakis, M. Fragiadakis, V. Plevris (eds.)
Corfu, Greece, 25–28 May 2011

AN IMPROVED DISPLACEMENT-BASED SEISMIC DESIGN METHODOLOGY FOR BRIDGES ACCOUNTING FOR HIGHER MODE EFFECTS

Andreas J. Kappos[1], **Konstantinos I. Gkatzogias**[1], **and Ioannis G. Gidaris**[1]

[1] Aristotle University of Thessaloniki
Laboratory of Reinforced Concrete & Masonry Structures, 54124, Greece
ajkap@civil.auth.gr; kgkatzog@gmail.com; igidaris31@gmail.com

Keywords: Displacement-Based Seismic Design, Bridges, Reinforced Concrete, Higher Mode Effects.

Abstract. *Weaknesses of existing methods for direct displacement-based design (DDBD) of bridges are pointed out and an improvement is suggested to account for higher mode effects, the key idea being not only the proper prediction of a target-displacement profile through the effective mode shape (EMS) method (wherein all significant modes are considered), but also the proper definition of the corresponding peak structural response. The proposed methodology is then verified by applying it to an actual bridge wherein the different pier heights and the unrestrained transverse displacement at the abutments result in an increased contribution of the second mode. A comparison between the extended and the 'standard' DDBD is conducted, while further issues such as additional design criteria leading to optimum design, the proper consideration of the degree of fixity at the pier's top, and the effect of the deck's torsional stiffness are also investigated. The resulting designs are evaluated using nonlinear response-history analysis (NLRHA) for a number of spectrum-compatible motions. Unlike the 'standard' DDBD, the extended procedure adequately reproduced the target-displacement profile providing at the same time a good estimate of results regarding additional design quantities such as yield displacements, displacement ductilities etc., closely matching the results of the more rigorous NLRHA. However, the need for additional iterations clearly indicates that practical application of the proposed procedure is feasible if it is fully 'automated', i.e. implemented in a software package.*

1 INTRODUCTION

Although force-based design methods still remain the norm in existing national seismic codes, during the past decade several research groups have developed alternative, performance-based, evaluation and design procedures [1], based directly on displacements and/or deformations. In this context, Moehle [2] proposed a general framework for earthquake-resistant design of structures based on drift control, with the seismic demand given by displacement response spectra, while Priestley and co-workers proposed the so-called direct displacement-based design (DDBD) for the design of fundamental mode dominated structures, which may be reduced to 'equivalent' linear single-degree-of-freedom (SDOF) systems [3 - 6]. The DDBD procedure starts from a target displacement, consistent with a deformation capacity ensured by an appropriate detailing of the structure. Estimating a reasonable value for the yield displacement, the target displacement translates into a displacement ductility demand and a corresponding equivalent damping ratio, which is used to reduce the selected displacement spectra, to account (indirectly) for non-linear hysteretic behaviour. Entering this response spectrum with the aforementioned target displacement (expressed in terms of the displacement of the equivalent SDOF system) the effective period (secant value at target displacement) of this system is determined; subsequently, the yield strength corresponding to the previously defined peak displacement and the secant stiffness calculated from the effective period, are found and used to apply a 'traditional' equivalent lateral force design of the structure. Calvi and Kingsley [7] were the first to extend this methodology to multi-degree-of-freedom (MDOF) structures which can be reduced to an equivalent SDOF system using an assumed deformed configuration of the structure. For buildings, this deformed configuration is that corresponding to a predefined plastic mechanism and is dominated by the fundamental mode. This version of the DDBD methodology, accompanied with tables for easier implementation of the procedure for different performance levels, was incorporated in the SEAOC [8] recommendations (referring only to buildings).

As far as bridges are concerned, the early work by Kowalsky et al. [5] dealing with isolated columns modelled as SDOF systems was later extended by Kowalsky [9] and Dwairi and Kowalsky [10], who introduced the effective mode shape (EMS) method to identify the displacement pattern and hence the displacement profile of a bridge at the beginning of the design process. Displacement pattern scenarios for continuous bridge structures subjected to transverse seismic excitation were also investigated in the latter study [10] through the use of nonlinear response-history analysis, while the recent study by Kappos et al. [11] identified required extensions and/or modifications of the aforementioned DBD procedure (see next section), for it to be applicable to actual bridges wherein the simplifying assumptions made at various stages of the procedure do not really hold. Finally, the book by Priestley et al. [12] presents a detailed treatment of the DBD procedure and its application to different structural types, mainly focussing on buildings, but also addressing bridges.

So far, the vast majority of the work performed on this topic does not consider higher mode effects, given the procedure's inherent limitation (resulting from the equivalent SDOF approach) to structures wherein the fundamental mode dominates the response. In a recent study, Adhikari et al. [13] introduced some additional considerations to account for higher mode effects on flexural strength of plastic hinges in the case of long-span concrete bridges with limited-ductile piers. Following the suggestion of Priestley et al. [12], Adhikari et al. used a response-spectrum analysis (RSA), after completion of the DDBD procedure, with two different design spectra (a 5%-damped design spectrum and a design spectrum with damping value obtained from the DDBD procedure) to determine the design responses (elastic and inelastic) at critical locations of the bridge as combinations of several modes.

In view of the aforementioned limitations of DDBD and the fact that bridges are structures wherein higher modes usually play a more critical role than in buildings, the present study attempts to refine and extend the procedure for bridges proposed by Dwairi and Kowalsky [10] and extended by the writers [11], to account for higher mode effects, not only regarding the proper definition of a target-displacement profile (comprising non-synchronous displacements, since all significant modes are considered), but also the proper definition of the corresponding peak structural response. The extended modal procedure proposed herein follows the general framework introduced in previous studies of Chopra and Goel [14] on buildings and Paraskeva et al. [15] on bridges, noting that these studies deal with the pushover procedure, rather than with design based on elastic analysis. The efficiency of the proposed methodology is then assessed by applying it to an actual bridge, whose different pier heights and the unrestrained transverse displacement at the abutments result in an increased contribution of higher modes. Some additional issues such as the proper consideration of the degree of fixity at the pier's top and the effect of the deck's torsional stiffness are also investigated, and comparisons between the extended modal and the 'standard' DDBD method are made. Design results are finally evaluated with the aid of nonlinear response-history analysis.

2 LIMITATIONS OF THE EXISTING DIRECT DBD PROCEDURE

The direct DBD method of Kowalsky [9] and Dwairi & Kowalsky [10] aims at designing a bridge to achieve a prescribed limit state that may be defined directly from displacements or derived from strain criteria under the selected design earthquake. The procedure utilizes the elastic displacement spectra reduced for an equivalent damping value, and the secant stiffness at the selected design displacement. Hence the stiffness of the bridge is not fixed at the beginning of the procedure (as in force-based design, FBD) but is derived in the process through the effective period (secant value). This is achieved by reducing the multi degree of freedom (MDOF) structure to an equivalent single degree of freedom (SDOF) system. The equivalent SDOF inelastic response is represented by the secant stiffness at peak response and equivalent damping, meant to account for hysteretic energy dissipation.

The crucial assumption involved in the above procedure is that this SDOF system suffices for capturing the displacement response of the bridge (which is typically inelastic, for all limit states beyond that corresponding to full serviceability); this implies that a single mode (which might, in fact, be a fictitious one, see subsequent sections) is used for deriving the properties of the equivalent SDOF system. The idea of the 'effective mode shape' (EMS) proposed in [9], building on concepts previously put forward by Calvi & Kingsley [7], is a useful one in this respect; it involves the estimation of a fictitious mode shape of the (inelastically responding) bridge by a statistical combination of individual modes. It is important to note that these modes are also fictitious ones, since they are not the (elastic) normal modes of the bridge but they are derived by eigenvalue analysis of a bridge model wherein yielding members (such as piers and, wherever applicable, abutments) are modelled with their secant stiffness at the intended displacement that generally exceeds the yield displacement, hence inelastic response is foreseen. It is clear from the foregoing summary of the procedure that, in general, a substantial number of iterations would be required to define effective mode shapes consistent with the inelastic response of the bridge to the design earthquake, even more so when multiple earthquake intensities are considered for checking multiple limit states (performance requirements). This important limitation of the method has been remedied to a certain extent by the 'calibration' of inelastic displacement patterns carried out by Dwairi & Kowalsky [10] who performed response-history analyses of four-span bridges with regular and irregular pier configurations, and with different support conditions at the abutments, for a set of 12 recorded motions from all over the world.

To simplify things and improve convergence of the procedure, the existing DDBD methodology assumes that the transverse response of single-column piers monolithically connected to the superstructure is that of a simple cantilever. This simplifying assumption can lead to conservative design of the piers, since the consideration that pier behaviour is that of a simple cantilever usually results to significant increase in the required steel ratio at the base of the pier. Additionally, the assumption of the simple cantilever implies that the superstructure has zero or significantly small torsional stiffness; in the common case of box-girder type decks this situation can be realistic only in the case of yielding of the superstructure's transverse reinforcement (Katsaras et al. 2009). However, this situation is not permitted by current seismic codes, wherein the superstructure is required to remain (essentially) elastic under the design earthquake. Moreover, proper consideration of the expected moment pattern in the piers has a significant importance in the case of the DBD procedure, as it affects the yield displacement (hence the displacement ductility demand) and the flexural stiffness of the piers. Although the previous aspects are identified by Priestley et al. [12], no specific guidelines are given for taking into account the degree of fixity at the pier's top.

A more general limitation of all DBD procedures is the (hardly ever mentioned in the previously cited publications on DBD) fact that not all bridges are, or should be made, displacement-controlled. There are two typical 'scenarios' wherein DBD is meaningless:

First, the case of regions of low, moderate, and even moderate-to-high seismic hazard, where the maximum displacement defined by the pertinent design spectrum is too low, even when no additional viscous damping (accounting for inelastic response) is introduced. Just as an example, seismic Zone I in Greece (which is the country with the highest seismicity in the European Union) is characterized by a design PGA=0.16g and a design spectrum, according to Eurocode 8 (CEN, 2005) for the common case of ground C, that results in a maximum elastic displacement (for 5% damping) of only 119 mm at a period T_D=2.0 sec (the Eurocode 8 recommended value for the threshold of the constant displacement branch of the spectrum). This is lower than the yield displacement of the pier of even a bridge with relatively short piers like the overpass reported later in the paper. In fact, to make DBD relevant to the common bridge configurations studied by the authors, higher seismic hazard (Zones II and III) and more conservative assumptions (T_D=4.0 sec) for the displacement spectrum had to be used. For bridges with (relatively) tall piers even these conservative assumptions cannot lead to meaningful DBD.

Second, the configuration of the bridge, including support conditions, which must also account for soil-structure interaction (SSI), should be such as to permit substantial displacements, accompanied by inelastic action. The case of bridges with tall piers has been mentioned previously, another case is that of bridges with transverse displacement blocked at the abutments. For instance, in the bridge studied in a later section, which is a typical overpass structure, blocking of transverse movement through stoppers at the (seat-type) abutments leads to very small displacements of the piers subsequent to their yielding, as most of the base shear developed after that stage goes to the abutments.

Last and not least, for DBD procedures for bridges to be suitable for practical design, they should be enriched with additional design criteria that would avoid the situation (that the authors have encountered on several occasions in their case-studies) wherein the advantages of DBD (with respect to FBD) are lost when minimum requirements for dimensioning and detailing of reinforced concrete (R/C) members are applied, in line with current practice.

The extensions to the Kowalsky et al. method introduced by the authors in [11] and here aim at remedying some of the aforementioned limitations.

3 PROPOSED EXTENSIONS TO THE 'STANDARD' DDBD

Various design criteria (complementary to those already included in the procedure of Kowalsky et al. and recently proposed by the authors [11]) are briefly reviewed herein; they can be deemed as guidelines that can assist the practicing engineer to achieve an efficient design, regarding both performance and economy. The extension (to account for higher-mode effects) of the displacement based design procedure for bridges with monolithically connected single-column piers to the superstructure, is then proposed, wherein the degree of fixity to pier top provided by superstructure rigidity is taken into consideration.

It is clear that not only the complexity but also the challenge of the design procedure derives from the multiplicity of 'solutions' to the design 'problem'. An ideal solution would satisfy all design criteria; nevertheless such an outcome (if at all feasible) would require numerous iterations. Therefore, the pragmatic approach is to meet as many criteria as possible with the least number of iterations. The additional design criteria proposed herein for the 'standard' DDBD method are as follows:

i. $V_{pier} \geq V(\rho_{req}=\rho_{min})$**:** The shear carried by each pier (V_{pier}) should exceed, for the sake of economical design, the shear (and hence the moment) that corresponds to the minimum required longitudinal reinforcement ratio, $V(\rho_{req}=\rho_{min})$. Otherwise, code minimum requirements will prevail and any benefits of DDBD will probably vanish.

ii. $V_{Abt} \leq V_u$**:** The shear carried by each abutment (V_{Abt}) should not exceed the ultimate shear (V_u), which is directly related to the 'weakest link' of the superstructure-abutment-backfill (SAB) system. For instance, in the case of a bearing-supported superstructure (with or without seismic links), it can be assumed that the SAB system will respond quasi-elastically ($K_{SAB} = K_{Bearings}$) until the closure of the gap between the deck and the abutment or seismic link; thus, V_u can be calculated from the ultimate force that can develop in the elastomeric bearings placed at the abutment, or the resistance of the seismic link. Activation of the abutment-backfill system can in turn determine V_u; this is also the 'weakest link' in the case of a monolithic superstructure-abutment connection.

iii. $k_{eff} \geq k(T_{eff}=T_D)$**:** Calculated supporting member (pier/abutment) secant stiffnesses (corresponding to the target-displacement profile), and hence the secant stiffness (k_{eff}) of the equivalent SDOF system (see Step 3 in next section) should not correspond to an effective period (T_{eff}) longer than the threshold (T_D) of the constant displacement branch of the design spectrum (see next section and Figures 2, 4). For very long T_{eff} the target displacement has to be reduced, which generally results in a longitudinal reinforcement increase and hence in less economical design. It should be stressed here that the choice of a proper T_D is essential for DDBD to be meaningful (see also section 'Evaluation of the proposed procedure in the case of an existing bridge').

iv. $\Delta_{pier} \leq \Delta_D$ and $\mu_{pier} \leq \mu_u$**:** The pier target-displacements should not exceed the corresponding 'damage-based' displacements (Δ_D), determined either from strain-based criteria [16] or drift-based criteria. P-Δ effects should also be considered. In addition, an ultimate displacement ductility value, determined by the designer (taking into account the detailing rules used in dissipating zones), should specify the upper limit in pier displacement ductilities.

v. $\Delta_{Abt} \leq \Delta_D$**:** As in design criterion (ii), the abutment target-displacements should not exceed the corresponding 'damage-based' displacements (Δ_D), defined with due consideration of the SAB system configuration. Referring to the common case of a bearing-supported superstructure, Δ_D is calculated in terms of the maximum acceptable shear strain ratio (γ_u), given the bearing horizontal stiffness.

In the extensions of the 'standard' DDBD method presented herein, the parameter of the equivalent cantilever length (h_{eq}), which is the distance from the pier base to the contraflexure point (see Fig. 1), is introduced to take into account the degree of fixity at the top of the pier.

Figure 1 represents the modelling of a pier with a rigid base and monolithically connected to the deck, whereas possible moment diagrams under transversal loading are also illustrated. It is obvious that a pier moment diagram consists of two different components; the bending moment derived from the inertial horizontal forces F, acting on the mass centroid (G), and the bending moment induced from the eccentricity of the latter forces with respect to the shear centre, in the usual case wherein the shear centre does not coincide with the mass centroid. The final moment diagram depends on the cracked torsional stiffness of the bridge deck, the superstructure-abutment connection and the pier-superstructure relative stiffness; likewise it is required to properly account for the degree of fixity at pier's top and hence for the pier's transverse response regarding its flexural stiffness (k_{pier}) and yield displacement ($\Delta_{y,pier}$), according to Equations (1) and (2), (referring to case (b) in Figure 1, similar relations can be derived for the other cases).

$$x_k = \frac{h_{eq}}{h} = \frac{h_{eq}}{h_{clear} + h_G}, \quad k_{eq} = \frac{3EI}{h_{eq}^{\,3}}, \quad k_{pier} = x_k k_{eq} \tag{1}$$

$$x_{\Delta y} = \frac{L_{eq}}{L_{eff}} = \frac{h_{eq} + 0.022 f_y d_{bl}}{h_{clear} + h_G + 0.022 f_y d_{bl}}, \quad \Delta_{y,eq} = \frac{\varphi_y L_{eq}^{\,2}}{3}, \quad \Delta_{y,pier} = \frac{1}{x_{\Delta y}} \Delta_{y,eq} \tag{2}$$

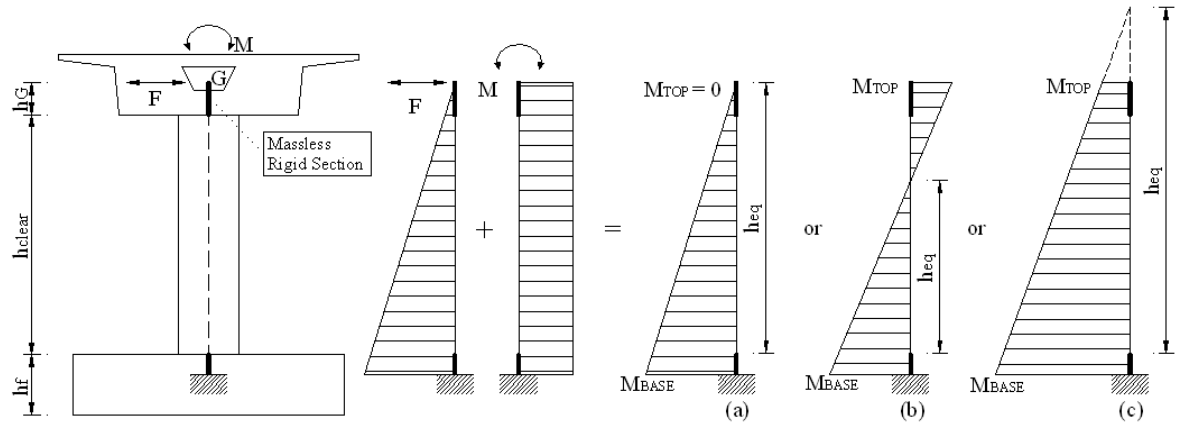

Figure 1: Pier modelling and transverse response accounting for the deck's torsional stiffness.

In Equations (1) and (2) E is the elasticity modulus of concrete and I is the moment of inertia of the pier cross-section (modified for cracking effects wherever necessary), φ_y is the yield curvature, f_y is the longitudinal bar yield stress and d_{bl} is the longitudinal bar diameter.

4 A MODAL DDBD PROCEDURE FOR BRIDGES

An extension of the DDBD methodology to bridge structures, wherein consideration of higher mode effects is deemed indispensable, is proposed herein. Procedures supplementary and/or alternative to those included in the 'standard' DDBD, are presented in this section, while an application of the suggested methodology to an actual bridge is given in the following section. For the sake of completeness (and the benefit of the reader) all steps of the procedure (including those that are essentially the same as in the 'standard' method [9, 10, 11]) are summarized in the following.

Step 0 - Definition of initial input parameters: General input parameters concerning the geometry (e.g. column height and diameter in piers with cylindrical columns), the mass properties (e.g. translational mass and mass moment of inertia), and material properties are defined. An initial estimate of the column cross-section is required. As a starting point, the output of the dimensioning of the deck and the piers for the Ultimate and Serviceability Limit States under the pertinent combinations of permanent and transient actions can be used. Then, single or multiple performance levels are set as design objectives, by designating the targeted damage states ('damage-based' displacements) for selected seismic hazard levels (elastic displacement response spectra).

Step 1 – Selection of the displacement pattern: The step prescribed in the 'standard' DDBD procedure, involves the computation of the relative pier-deck stiffness (RS) and the determination of whether the bridge has a rigid or a flexible displacement pattern, as suggested by Dwairi et al. [10]. Given that the procedure proposed here is intended for bridges where higher mode contribution should not be ignored, the flexible displacement pattern scenario is adopted, disregarding the relative stiffness parameter. This means that this step is essentially redundant, nevertheless it is deemed advisable to retain it, as it is always useful for the designer to have a proper indication of the relative stiffness of the deck.

Step 2 – Definition of target-displacement profiles: The iterative effective mode shape (EMS) method is followed, according to the following steps:

i. Evaluation of mode shapes *(Φ_j)*: Due to the unavailability of the member effective properties at the start of the process a first estimation is required. Based on current seismic design practice for bridges it can be assumed that the superstructure will respond essentially elastically, regarding its flexural stiffness, while for its torsional stiffness it is proposed to assume 20% of the uncracked value, based on the ratios (10÷30%) of cracked-to-uncracked torsional stiffness just after concrete cracking, estimated by Katsaras et al. [17]. On the other hand, it is suggested that a secant flexural stiffness equal to 10%EI_g be applied to columns expected to deform inelastically, while 60% of the uncracked section stiffness is suggested for columns that are expected to remain elastic. The reduction in the effective axial [18] and shear [19] stiffness of the column(s) can be considered proportional to the reduction in the effective flexural stiffness. Once the structure properties have been established, the eigenvalue problem can be solved, hence the mode shapes Φ_i can be obtained.

ii. Evaluation of modal participation factors *(Γ_j)*: The modal participation factors can be computed using standard procedures, i.e. Equation (3), where $\boldsymbol{m}$ represents a diagonal mass matrix and $\boldsymbol{\iota}$ is a unit vector.

$$\Gamma_j = \frac{\boldsymbol{\Phi}_j^T \boldsymbol{m} \boldsymbol{\iota}}{\boldsymbol{\Phi}_j^T \boldsymbol{m} \boldsymbol{\Phi}_j} \tag{3}$$

iii. Evaluation of peak modal displacements *($u_{i,j}$)*: The peak modal displacements are computed according to Equation (4), where index i represents the joint number associated with a lumped mass, as per the inertial discretization, index j represents the mode number, $\Phi_{i,j}$ is the modal factor of joint i and mode j, and S_{dj} is the spectral displacement for mode j obtained by entering the 5%-damped design spectra with the period obtained from modal analysis.

$$u_{i,j} = \Gamma_j \Phi_{i,j} S_{dj} \tag{4}$$

iv. Evaluation of expected displacement pattern: The displacement pattern (δ_i) is obtained by an appropriate combination of the peak modal displacements, such as the SRSS combination given by Equation (5); CQC combination is expected to yield better results when the natural frequencies of the participating modes in the response are closely spaced.

$$\delta_i = \sqrt{\sum_j u^2_{i,j}} \tag{5}$$

It is noted that a displacement pattern derived from the above procedure accounts for the effect of all significant modes (e.g. those needed to capture 90% of the total mass in the transverse direction); therefore, it does not correspond to an actual inelastic deformed shape of the bridge, particularly so in the case of asymmetric systems. To obtain the target displacement profile (Δ_i), the displacement pattern given by Equation (5) is scaled such that none of the member (pier or abutment) displacements exceed the target displacements obtained based on strain or drift criteria:

$$\Delta_i = \delta_i \frac{\Delta_{D,c}}{\delta_c} \tag{6}$$

where $\Delta_{D,c}$ and δ_c are the 'damage-based' displacement and the modal value at the critical mass c (whose displacement governs the design), respectively. Finally, peak modal displacements ($u_{i,j}$) are scaled to N modal target-displacement profiles ($U_{i,j}$) utilizing the same scaling coefficient as that used to obtain the target-displacement profile in Equation (6):

$$U_{i,j} = u_{i,j} \frac{\Delta_{D,c}}{\delta_c} \tag{7}$$

An immediate consequence of the aforementioned procedure is that the combination of the N modal target-displacement profiles ($U_{i,j}$) yields the target-displacement profile (Δ_i); hence, in the case the SRSS combination rule is used:

$$\Delta_i = \sqrt{\sum_j U^2_{i,j}} \tag{8}$$

Step 3 – Definition of N+1 equivalent SDOF structures: These structures are established based on equal work done by the MDOF bridge and the equivalent SDOF structure, according to Calvi & Kingsley [7]. Each of the N SDOF structures is related to the corresponding modal target-displacement profile ($U_{i,j}$), whereas the additional SDOF is related to the target-displacement profile (Δ_i). Utilizing Equations (9) and (10), an equivalent system displacement (Δ_{sys}, $U_{sys,j}$), mass (M_{sys}, $M_{sys,j}$) and location (x_{sys}, $x_{sys,j}$) of the SDOF across the MDOF bridge deck is computed for each of the $N+1$ SDOF structures. In Equations (9) and (10), m_i is the mass associated with joint i, and n is the number of joints as per the inertial discretization.

$$U_{sys,j} = \frac{\sum_{i=1}^{n} m_i U^2_{i,j}}{\sum_{i=1}^{n} m_i U_{i,j}},\ M_{sys(j)} = \frac{\sum_{i=1}^{n} m_i U_{i,j}}{U_{sys,j}},\ x_{sys,j} = \frac{\sum_{i=1}^{n} \left(m_i U_{i,j} x_i \right)}{\sum_{i=1}^{n} \left(m_i U_{i,j} \right)} \tag{9}$$

$$\Delta_{sys} = \frac{\sum_{i=1}^{n} m_i \Delta_i^2}{\sum_{i=1}^{n} m_i \Delta_i},\ M_{sys} = \frac{\sum_{i=1}^{n} m_i \Delta_i}{\Delta_{sys}},\ x_{sys} = \frac{\sum_{i=1}^{n} \left(m_i \Delta_i x_i \right)}{\sum_{i=1}^{n} \left(m_i \Delta_i \right)} \tag{10}$$

Step 4 – Estimation of equivalent viscous damping levels: Utilizing the target displacement (Δ_i) and the modal target-displacement profiles ($U_{i,j}$), the ductility level is calculated for each member (for each of the $N+1$ profiles), according to Equation (11) and in line with the equivalent cantilever concept (Equation (2)). The height of the equivalent cantilever cannot be determined at the initial stage of design, therefore either preliminary structural analyses should be performed for each of the $N+1$ equivalent structures under lateral loads compatible with the corresponding profile, or an assumption that the height of the equivalent cantilever equals the height of the pier, should be made during the first iteration. The first approach is strongly recommended for the case of significant higher mode effects, since it reduces the number of iterations required to achieve convergence.

$$\mu_{\Delta_i} = \Delta_i/\Delta_{yi},\ (or\ \mu_{\Delta_i} = U_{i,j} / \Delta_{yi,j}) \tag{11}$$

Yield curvatures in Equation (2) are estimated using Equation (12), where ε_y is the reinforcement yield strain and D is the diameter of a circular section; similar equations are provided for different section shapes [12, 19].

$$\varphi_y = 2.25\varepsilon_y/D \tag{12}$$

The displacement ductility ($\mu_{\Delta,i}$) of each pier should be compared with μ_u, (see design criterion iv). If any $\mu_{\Delta,i}$ exceeds μ_u, the designer should revise either the target-displacement profile (by reducing the pier limit-state displacements) or the yield displacements (by reducing the pier cross-section).

Several relationships [20 - 23] between hysteretic damping and ductility have been proposed. The one obtained by Dwairi [20] based on Takeda's hysteretic model [24], given by Equation (13), is used here. Additional elastic viscous damping (ξ_v) up to 5% should be added to the hysteretic damping in line with the approach proposed by Grant et al. [25].

$$\xi_i = \xi_v + \frac{50}{\pi}\left(\frac{\mu_\Delta - 1}{\mu_\Delta}\right)\% \tag{13}$$

These damping values need to be combined in some form to obtain system damping for each of the $N+1$ equivalent SDOF structures. A weighted average can be computed, as given by Equation (14), where $W_i / \Sigma W_k$ is a weighting factor, based on the work (W_i) done by each member (Equation (15)), according to the Kowalsky [9] approach.

$$\xi_{sys} = \sum_{i=1}^{n}\left(\frac{W_i}{\sum_{k=1}^{n} W_k}\xi_i\right),\ \ \xi_{sys(j)} = \sum_{i=1}^{n}\left(\frac{W_{i,j}}{\sum_{k=1}^{n} W_{k,j}}\xi_{i,j}\right) \tag{14}$$

$$W_i = V_i\Delta_i,\ \ W_{i,j} = V_{i,j}U_{i,j} \tag{15}$$

Calculation of the weighting factors obviously requires the knowledge of member forces (V), which are not known at the current step. As a starting point, it can be assumed that the seismic force carried by the abutments is equal to 30% of the total seismic force carried by the bridge and column shears are inversely proportional to column heights, as illustrated by Equation (16) [9], where μ is less than one for elastic columns and equal to one for columns that have yielded. In subsequent iterations, system damping is computed in proportion to the member forces obtained from structural analyses.

$$W_i = \mu_{\Delta_i}\Delta_i/h_{eq,i},\ W_{i,j} = \mu_{\Delta_i}U_{i,j}/h_{eq,ij} \tag{16}$$

Step 5 – Determination of the equivalent structures effective periods: Utilizing the *N+1* system target-displacements (Δ_{sys}, $U_{sys,j}$), levels of system damping (ξ_{sys}, $\xi_{sys,j}$), and elastic response spectra for the chosen seismic demand, the effective periods (T_{eff}, $T_{eff,j}$) of the equivalent structures are determined from the design spectrum as shown in Figure 2.

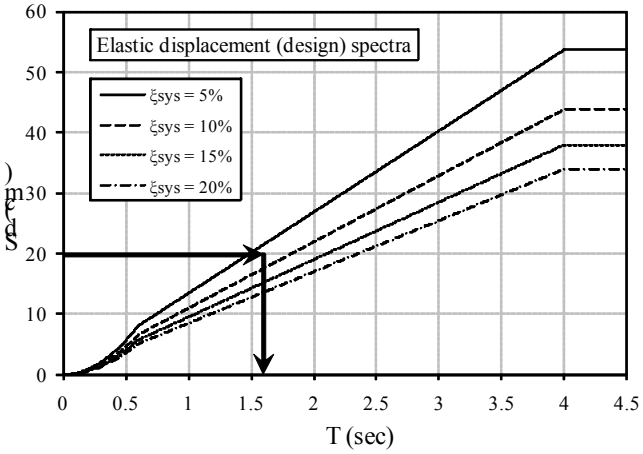

Figure 2: Effective period evaluation based on DDBD procedure.

Once again, revision of the target-displacement profile is required when the calculated target displacements exceed the displacement that corresponds to the corner period (T_D) (see design criterion iii). Once the effective periods have been determined, effective stiffnesses (k_{eff}, $k_{eff,j}$) and design base shears (V_B, $V_{B,j}$) are computed by Equations (17) and (18), respectively.

$$k_{eff} = 4\pi^2 M_{sys}/T_{eff}^2,\ k_{eff,j} = 4\pi^2 M_{sys,j}/T_{eff,j}^2 \tag{17}$$

$$V_B = k_{eff}\Delta_{sys},\ V_{B,j} = k_{eff,j}U_{sys,j} \tag{18}$$

Step 6 – Verification of design assumptions: Design base shears (V_B, $V_{B,j}$) are distributed in proportion to the inverse of the column height according to Equation (19), which is based on the simplifying assumption that all columns have the same diameter and longitudinal reinforcement steel ratio, zero post-elastic slope of the force-displacement response, mass small enough such that inertia forces due to self-weight can be neglected, and the same end-fixity conditions. In Equation (19) μ_i and μ_k are less than one for elastic columns and equal to one for columns that have yielded and F_{Abt} represents the total force carried by the abutments. Member cracked section stiffnesses are computed for each of the *N+1* profiles, using Equations (20) and are compared to assumed values of Step 2. If the values related to the target-displacement profile (Δ_i) differ significantly, computed secant stiffnesses ($k_{eff,i}$) are utilized in the EMS to obtain revised target-displacement profiles (Δ_i, $U_{i,j}$). Steps 2 to 6 are repeated by changing column secant stiffnesses until the target profile (Δ_i) stabilizes. Although a strict approach requires iteration within Steps 2 to 6 until all profiles (Δ_i and $U_{i,j}$) stabilize, the implementation of the proposed methodology in the next section indicates that whenever Δ_i stabilizes, $U_{i,j}$ are also practically stabilized, hence Δ_i can be used as the sole convergence criterion.

$$V_{B,k} = \left(V_B - F_{Abt}\right)\frac{\mu_{\Delta,k}}{h_k}\Bigg/\sum_{i=1}^{n}\frac{\mu_{\Delta,i}}{h_i},\ V_{B,kj} = \left(V_{B,j} - F_{Abt,j}\right)\frac{\mu_{\Delta,kj}}{h_k}\Bigg/\sum_{i=1}^{n}\frac{\mu_{\Delta,ij}}{h_i} \tag{19}$$

$$k_{eff,i} = V_{B,i}/\Delta_i,\ k_{eff,ij} = V_{B,ij}/U_{i,j} \tag{20}$$

Step 7 - Structural analysis: Once the target-displacement profile (Δ_i) stabilizes, base shears ($V_{B,j}$) are distributed as inertia forces to the masses of the MDOF structure in accordance with the modal target-displacement profiles ($U_{i,j}$), as given by Equation (21) [7]. In this equation $F_{i,j}$ are the bent inertia forces, $V_{B,j}$ are the design base shears, indices i and k refer to joint numbers, and n is the number of joints.

$$F_{k,j} = V_{B,j}\left(m_k U_{i,j}\right) \Big/ \sum_{i=1}^{n}\left(m_i U_{i,j}\right) \tag{21}$$

N structural analyses (as many as the significant modes) are performed on the bridge under the inertia loads, to obtain the 'modal' base shear for each column. Secant stiffnesses $k_{eff,ij}$ obtained from the iteration within Step 6, at which stabilization of Δ_i (hence stabilization of $U_{i,j}$ as mentioned in Step 6) was observed, should be used in each of the N structural model analyses, in order to be consistent with the DDBD philosophy. Afterwards, displacements derived from the N structural analyses are compared with the corresponding profiles $U_{i,j}$. In the case of significantly different displacements, reasonable values for column secant stiffnesses are assumed and analyses are conducted until convergence is achieved. Once the displacement profiles obtained from structural analyses converge to the assumed modal target-displacement profiles, column secant stiffnesses and abutment forces from each analysis are compared with the values assumed at Step 6, at which stabilization of $U_{i,j}$ was achieved. It is reminded that during the first loop of iterations the seismic force carried by the abutments is assumed equal to 30% of the total seismic force carried by the bridge for all the $N+1$ cases. In case of significant discrepancy, the target-displacement profile is revised utilizing the EMS method and forces from structural analyses. Steps 2 to 7 are repeated, until column secant stiffnesses and abutment forces converge.

In order to perform the new loop of iterations and the new EMS in particular, previous loop secant stiffnesses ($k_{eff,i}$) (Step 6) can be assumed as a starting point. Furthermore, revised equivalent cantilever heights are computed according to the results of the N structural analyses, which were previously performed, as far as the modal target-displacement profiles ($U_{i,j}$) are concerned, whereas in the case of the target-displacement profile (Δ_i), proper values of the equivalent cantilever heights can be approximately determined by combining the peak 'modal' responses (N structural analyses). Following the same approach, the force carried by the abutments and the base shear distribution for each of the $N+1$ cases required in the subsequent steps are determined from analysis results, instead of utilizing Equation (19), which, given the diversity of the column end-fixity conditions, is not accurate.

Step 8 - Design of the MDOF structure: The MDOF bridge is designed in accordance with capacity design principles and also design criterion (i), such that the desired failure mechanism, as well as economical design are achieved. The response quantities of design interest (displacements, plastic hinge rotations, internal pier forces) are determined by combining the peak 'modal' responses (the N structural analyses), using an appropriate modal combination rule (e.g. SRSS or CQC), superimposed with the pertinent combinations of permanent and transient actions. To meet design criterion (i) the target-displacement profile and/or the pier cross section are revised and Steps 1 to 8 are repeated.

5 EVALUATION OF THE PROPOSED PROCEDURE IN THE CASE OF AN EXISTING BRIDGE

5.1 Description of studied bridge

To investigate the accuracy, efficiency, and also the practicality, of the proposed procedure it was deemed appropriate to apply it to an actual bridge structure, whose different pier heights and the unrestrained transverse displacement at the abutments result in an increased contribution of the second mode. The selected structure (known as the T7 Overpass), is quite common in modern motorway construction in Europe. The 3-span structure of total length equal to 99 m (see Figure 3), is located in northern Greece and is characterized by a significant longitudinal slope (approximately 7%). The deck consists of a 10 m wide prestressed concrete box girder section with a variable geometry across the longitudinal axis of the bridge (see Figure 3). The two piers have a cylindrical cross section, a common choice for bridges both in Europe and in other areas, while the pier heights are unequal (clear column height of 5.94 and 7.93 m), due to the deck's longitudinal inclination. The deck is monolithically connected to the two piers, while it rests on its abutments through elastomeric bearings; movement in both the longitudinal and the transverse direction is initially allowed at the abutments, but transverse displacements are restrained in the actual bridge whenever the 15 cm gap shown in Figure 3 is closed. In applying the proposed design procedure to this bridge, the gap size, as well as the characteristics of the bearings are treated as design parameters. The piers and the abutments are supported on surface foundations (footings) of similar configuration.

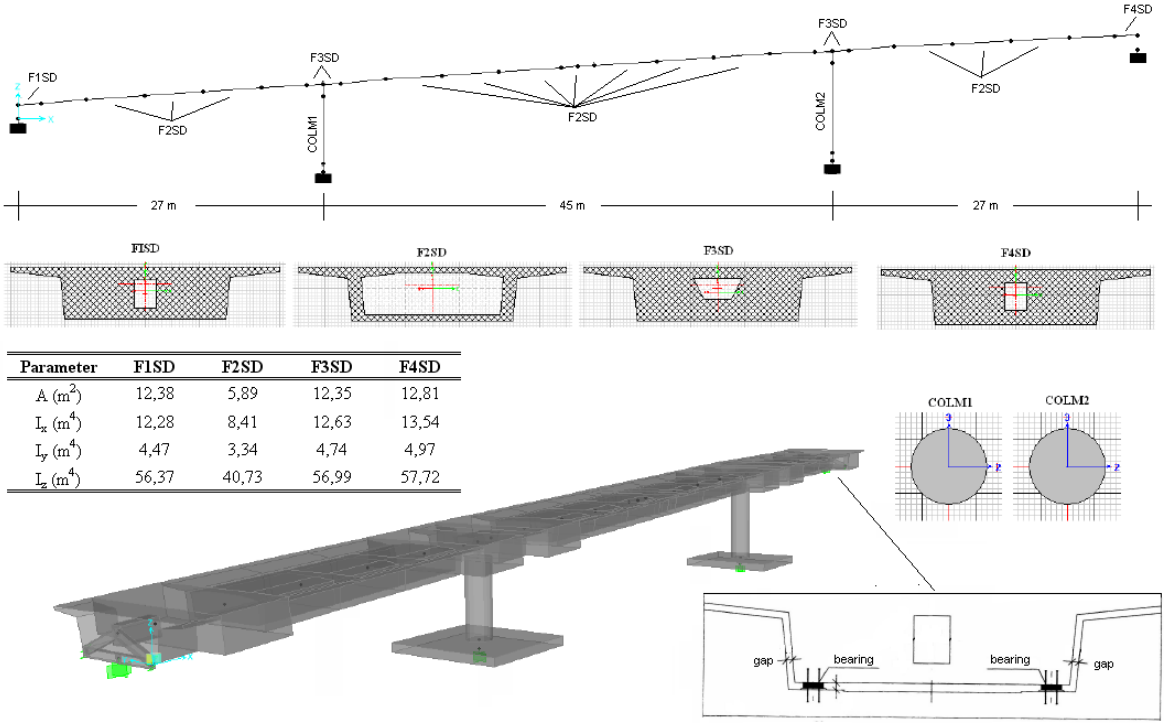

Parameter	F1SD	F2SD	F3SD	F4SD
A (m^2)	12,38	5,89	12,35	12,81
I_x (m^4)	12,28	8,41	12,63	13,54
I_y (m^4)	4,47	3,34	4,74	4,97
I_z (m^4)	56,37	40,73	56,99	57,72

Figure 3: Layout of the bridge configuration and finite element modelling.

T7 Overpass was designed using DDBD, both in the form proposed by Dwairi and Kowalsky [10], and its modified version proposed herein, for two different seismic zones. The Greek Seismic Code (EAK2000) elastic spectrum [26] for Zone II (PGA of 0.24*g*) and III (PGA of 0.36*g*) was the basis for seismic design; it corresponded to soil conditions category 'B' of the Code, which can be deemed equivalent to subsoil class 'B' of older drafts of Eurocode 8-2 and

closer to 'C' in the final version of the Eurocode [27]. The bridge was designed as a ductile structure implying that plastic hinges are expected to form in the piers, while P-Δ effects were taken into consideration. A further parameter that was investigated in applying the DDBD was the effect of the girder's torsional stiffness.

In the analyses presented in the following, the focus is on the transverse response of the bridge, as it is well known (e.g. Reference [28]) that this is the response most affected by higher modes; additional analyses in the longitudinal direction were also conducted [29], however due to space limitations and the fact that longitudinal design was found to be less critical, these analyses are not presented herein. The analysis was carried out using the SAP2000 software [30]; the reference finite element model (Fig. 3) involved 32 non-prismatic 3D beam elements. Preliminary analyses accounting for soil-structure interaction (SSI) effects, using an appropriate foundation compliance matrix, have shown that due to the relatively stiff soil formations underneath the studied bridge, SSI had little effect on the response; hence these effects were subsequently ignored in the design (and assessment) of the bridge.

5.2 'Standard' direct displacement-based design (DDBD)

A 'standard' DDBD [9, 10, 11] was first performed, mainly to show the inefficacy of the procedure, which arises from its inherent restriction to structures wherein the fundamental mode dominates the response, as previously pointed out by Calvi & Kingsley [7]. In the case of T7 Overpass, the transverse response is determined by two dominant modes (see Figure 5). A 'damage control' limit state that corresponds to a drift ratio of 3%, was considered; qualitatively, 'damage control' implies that only repairable damage occurs in the columns. The design displacement spectrum was derived from the pertinent elastic acceleration response spectrum (see Figure 4), using the well-known equation $S_d(T) = S_a(T)/\omega^2$

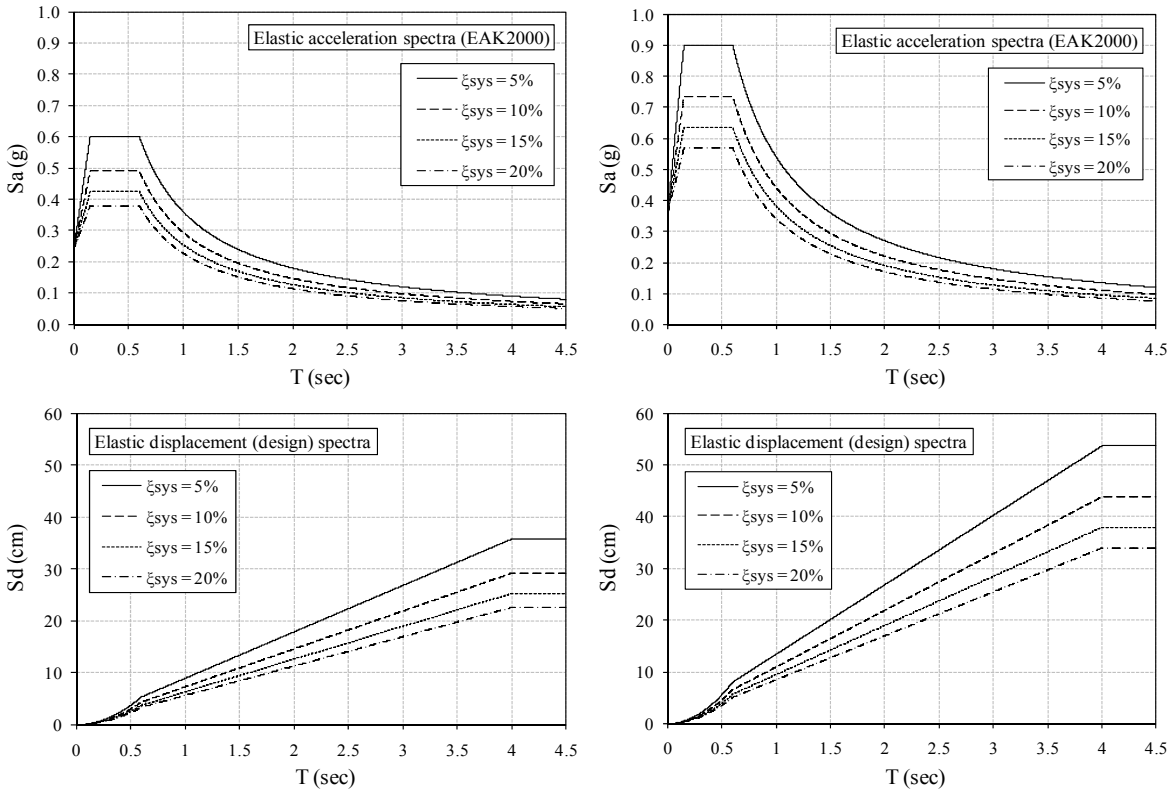

Figure 4: Elastic acceleration (according to EAK2000, Soil Type B) and displacement response spectra; left: Zone II (PGA=0.24*g*), right: Zone III (PGA=0.36*g*).

A significant modification was made to the spectrum used for design, i.e. the corner period in S_d was taken equal to 4.0 sec, according to SEAOC's [8] recommendations, which is substantially higher than the values of 2.5 and 2.0 specified by EAK2000 and EC8, respectively. This modification is not only in line with recent research findings, but also necessary for DDBD to be meaningful (short corner periods lead to small displacement values in the period range that is common to DDBD, which relies on secant stiffness values at the maximum displacement). Moreover, the modification to the elastic acceleration spectrum, required to account for ductile response through an increased effective damping ratio, was made using the damping modifier (η) adopted in the final version of EC8, i.e. Equation (22) below, where ξ_{sys} is the viscous damping ratio of the structure, expressed as a percentage.

$$\eta = \sqrt{10/(5+\xi_{sys})} \tag{22}$$

As previously mentioned, the mechanical characteristics of the elastomeric bearings are a design parameter, hence an initial estimate is required. A rational choice of the elastomer (rubber) cross-sectional area can be made from the design for axial loading, while, regarding the transverse modes of the bridge (Figure 5), the total thickness (t_r) of the elastomer should provide the target-displacement profile with adequate displacements at the abutments, so that the 'damage-based' displacements (Δ_D) of each column, related to the acceptable drift ratio, could be attained, and a reasonable longitudinal reinforcement ratio could be obtained for the pier. The elastomeric bearings chosen herein are rectangular in shape (350 · 450 mm) with t_r of 88 mm, horizontal stiffness of 2506 kN/m and equivalent viscous damping ratio equal to 5%; two bearings are placed at each abutment, as shown in Figure 3. The maximum acceptable shear strain ratio (γ_u), from which the 'damage-based' displacements of the bearings are derived, is taken equal to 2.0. Introducing the 3% drift ratios for the columns, the 'damage-based' displacements of all members (piers or abutments) were calculated and are shown in Table 1; a diameter of 2.0 m was initially assumed for the two columns.

Damage-based displacements				
Member	Abt_1	$Col._1$	$Col._2$	Abt_2
Δ_D (m)	0.176	0.218	0.278	0.176

Table 1: 'Damage-based' displacements related to the 'damage control' limit state.

In order to obtain the target-displacement profile for the inelastic system, the EMS method was utilised. It was assumed that the superstructure will respond essentially elastically, as far as its flexural stiffness is concerned, while its torsional stiffness was set equal to 20% of the uncracked section torsional stiffness [17]. A secant flexural stiffness equal to 10% the gross value was applied to the columns (both of them are expected to deform inelastically), while the reduction in the effective axial and shear stiffness was considered to be proportional to the reduction in flexural stiffness. Figure 5 illustrates the target-displacement profile derived from applying the EMS repeatedly until convergence was achieved (four iterations were needed in total); displacement patterns, peak modal displacements and modal mass participation factors for each mode are also shown. Convergence was checked with regard to stabilization of the target-displacement profile or the column secant stiffness from one iteration to the next. Discrete dots on the graphs represent the points of the deck's axis passing from its mass centroid, corresponding to the centres of elastomeric bearings and columns.

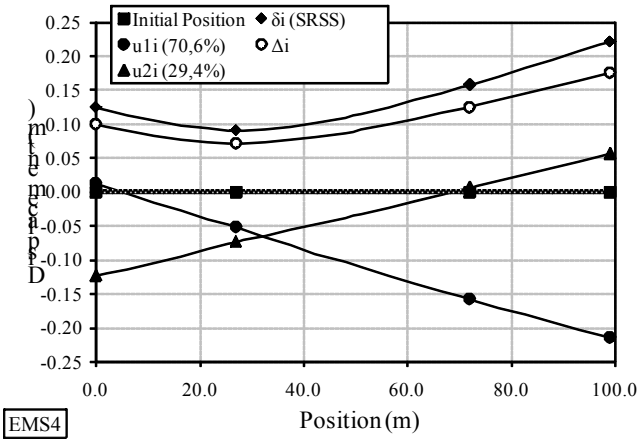

Figure 5: Displacement profile: Peak modal displacements $u_{i,j}$, displacement pattern δ_i and target-displacement profiles Δ_i, estimated iteratively from EMS method.

The next step of the 'standard' DDBD method involves structural analysis of the bridge under the inertia loads given by Equation (21), (where, in the 'standard' procedure $U_{i,j}$ corresponds to Δ_i), to obtain the design base shear of each column. In Figure 6 the displacement profile derived from structural analysis Δ_i (SA1), is compared with the target-displacement profile Δ_i (EMS4). The discrepancy between the two profiles reveals one of the main deficiencies of the standard DDBD, i.e. its inability to predict the peak structural response (in terms of displacements and hence internal member forces), on the basis of which design will be carried out.

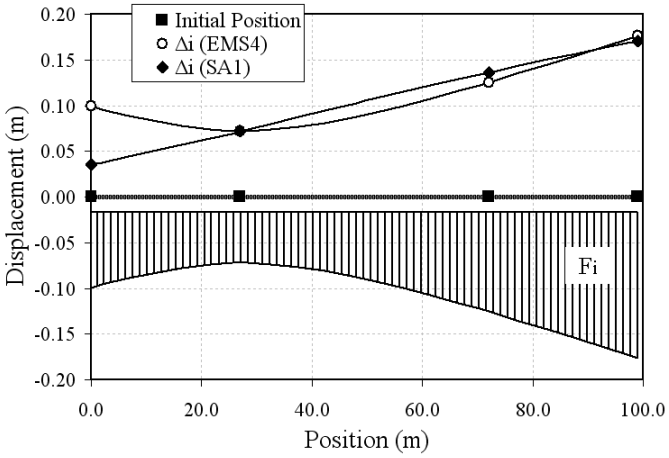

Figure 6: Structural analysis displacement profile (SA1) compared with target-displacement profile (base shear distribution (F_i) as inertia forces to the masses of the MDOF structure is also illustrated).

The target-displacement profile, which generally reflects the ultimate limit state (in terms of displacements) of the structural members, was constructed from the combination of the peak modal displacements (according to the SRSS rule), and then scaled in such a way that none of the member displacements exceeds the 'damage-based' design values. By following this procedure, the target-displacement profile never reflects an actual deformed shape of the structure; instead, it represents a fictitious deformed shape comprised of non-simultaneous displacements, which is deemed to reflect the peak (and non-simultaneous) structural member response. Therefore, in cases (like here) where more than one mode dominates the response, a static structural analysis under a modal combination of seismic lateral forces such as those

given by Equation (21) (whose distribution is also shown in Figure 6), cannot, under any circumstances, produce the target-displacement profile.

A final remark regarding the above, is that the above discrepancy in the displacement profiles is due neither to errors in the estimation of the equivalent cantilever heights nor to the approximate base shear distribution according to Equation (19). In fact, additional iterative structural analyses wherein secant stiffnesses are modified, as required by the DDBD, in this case can only lead to convergence in terms of one critical member displacement (the first member that reaches its limit state) rather than in terms of the entire target-displacement profile, which is determined from the contribution of all significant modes.

5.3 Modal direct displacement-based design (MDDBD)

The proposed extended DDBD procedure was applied to the T7 Overpass as follows.

Step 0: As in the 'standard' DDBD, a 2.0 m column diameter was assumed as a starting point. However, seismic design for Zone II resulted in column longitudinal reinforcement ratios less than the minimum required by E39 [18] and other codes. Due to the fact that providing the minimum required ratio, would obscure the concepts of DDBD (regarding the target profile, displacement ductilities etc.) and aiming at an optimum design (see design criterion i), a 1.5 m column diameter was subsequently used. Preliminary structural analyses were performed for each of the three equivalent SDOF systems (N+1, considering the first 2 modes), under lateral loads compatible with the modal profiles and their SRSS combination, to obtain the equivalent cantilever heights and the uncracked stiffnesses ($K_{g,i}$), according to Equation (1). The assumed characteristics of the elastomeric bearings, the design spectrum and the 'damage-based' displacements were determined as in the standard DDBD.

Steps 2 to 6: The previously described EMS methodology was applied. In order to establish the initial displacement profiles, a modal analysis was conducted where member stiffnesses were set as in the standard DDBD. The peak modal displacements ($u_{i,j}$), the displacement pattern (δ_i), the target-displacement profile (Δ_i) and the modal target displacements profiles ($U_{i,j}$) were determined by Equations (4 to 7) respectively, and presented herein in Figure 7, and it is clear that the abutments are the critical elements. The three equivalent SDOF systems were defined in accordance with Equations (9) and (10).

Once the target-displacement profiles were established, the individual member ductility values (Equations (11)) were calculated along with the corresponding equivalent viscous damping values (Equation (13)), where elastomeric bearings were assumed to respond elastically (ξ_{Abt}=5%). Assuming that 30% of the total shear is carried by the abutments (in all 3 cases), the equivalent system damping values were obtained from Equations (14) and (16) for the first iteration and Equation (15) thereafter. The effective periods at maximum response were then obtained from Figure 4. This was then followed by the calculation of secant stiffnesses at maximum response (Equation (17)). Design base shears were calculated from Equation (18) and member shear forces from Equation (19). It is noted, that in the case of modal target-displacements with different signs, Equation (23) was used in lieu of (19).

$$V_{B,j} - F_{Abt,j} = V_{B,1j} + V_{B,1j}, \quad V_{B,1j} / V_{B,2j} = -\left(\frac{\mu_{\Delta,1j}}{h_{eq,1j}} \Big/ \frac{\mu_{\Delta,2j}}{h_{eq,2j}} \right) \tag{23}$$

As soon as base shears for the SDOF systems are defined, the fraction of the shear carried by the abutments can be recalculated using the following equation

$$x_{Abt}(\%) = F_{Abt}/V_B = \sum F_{Abt,i}/V_B = \sum\left(2k_h\Delta_{Abt,i}\right)/V_B$$
$$x_{Abt,j}(\%) = F_{Abt,j}/V_{B,j} = \sum F_{Abt,ij}/V_{B,j} = \sum\left(2k_h\Delta_{Abt,i}\right)/V_{B,j} \quad (24)$$

In Equation (24), k_h represents the bearing's horizontal stiffness (for one bearing). If the revised fractions differ significantly from the assumed values (30%), Steps 4 and 5 are repeated until fractions of x_{Abt} stabilize. It is clear than in the case of seat-type abutments with bearings the design is simplified on the grounds that the shear carried by the abutment is known from the first iteration. The column secant stiffness values can be recalculated at this point since column forces and member displacements are now known (Equation (20)). This is then followed by a revised modal analysis with the new secant stiffness properties resulting into new target-displacement profiles (Δ_i, U_{ij}). In total, four iterations were needed until Δ_i stabilized. The finally derived (from all iterations) profiles are illustrated in Figure 7. It is evident (from Iterations 3 and 4), that whenever Δ_i stabilizes, $U_{i,j}$ also stabilize.

Step 7: Once the target-displacement profile (Δ_i) stabilized, two structural analyses of the MDOF structure were performed under the inertia forces of Equation (19), utilizing the secant stiffnesses ($k_{eff,ij}$) from the 4th Iteration. Due to the inconsistency of the derived displacements ($U_{an,ij}$) with the corresponding modal target-displacements ($U_{i,j}$), the two analyses were repeated with revised secant stiffnesses until convergence was achieved. Since the final secant stiffnesses of columns differed significantly from the assumed ones, Steps 1 to 7 were repeated, so long as new equivalent cantilever heights and column shear distribution were defined from the results of the structural analyses.

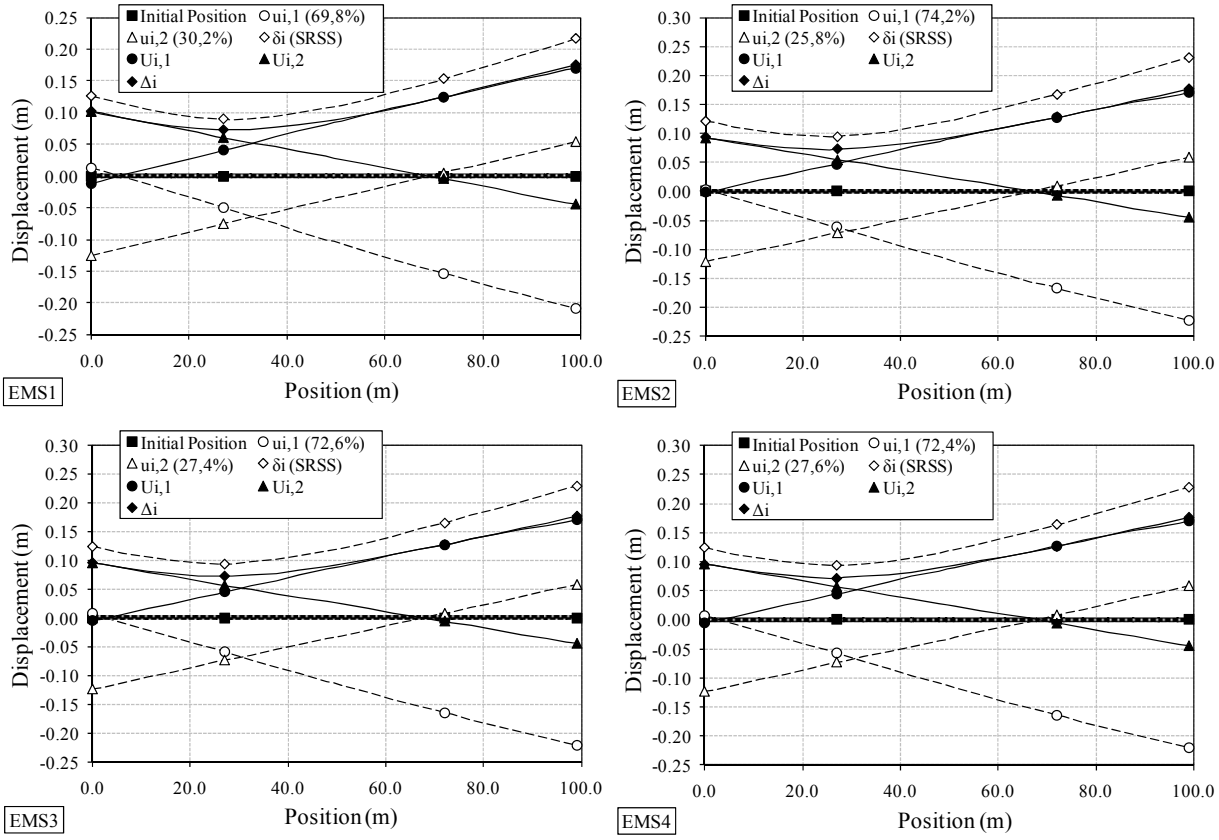

Figure 7: Displacement profiles: Peak modal displacements $u_{i,j}$, displacement pattern δ_i, modal target-displacement profiles $U_{i,j}$ and target-displacement profiles Δ_i, successively derived from EMS.

The new loop of iterations attempts to reduce the discrepancy resulting from the equivalent cantilever height updating (which does not change much the initially assumed value), and the shear distribution effect according to Equation (19), but not the fraction of the shear carried by the abutments, since this is considered known, as already discussed. The results from the final iterations are summarised in Figure 9(a) in the next section, where the target-displacements profiles (Δ_i) and the profiles derived from structural analysis ($\Delta_{i,an}$) are shown. It is noted that $\Delta_{i,an}$ is derived from the SRSS combination of $U_{ij,an}$.

Step 8: The response quantities of design interest (rotations, pier forces) are determined by combining the peak 'modal' responses (from the two structural analyses), using the SRSS combination rule, superimposed with the pertinent combinations of permanent and transient actions. P-Δ effects were also taken into account, and it is verified that the stability index satisfied $\theta_\Delta \leq 0.20$. Finally, the design procedure yielded a longitudinal steel ratio of 9.8‰ and 12.4‰ for Col_1 and Col_2, respectively. The ratio of Col_1 is just slightly less than the minimum required ratio (1%), according to E39 and the Eurocode.

The whole procedure was repeated for the case of Zone III, (PGA of 0.36*g*), in which case a 2.0 m column diameter was selected. The target-displacements profiles (Δ_i) and the profiles derived from structural analysis ($\Delta_{i,an}$) are shown in Figure 9(b). In this case the design procedure yielded a longitudinal steel ratio of 11.5‰ and 19.0‰ for Col_1 and Col_2, respectively.

Furthermore, the effect of the girder's torsional stiffness throughout the suggested methodology was investigated. The design procedure was repeated assuming zero deck torsional stiffness, which results to cantilever action of the columns (see Figure 1(a)), and using a simplified stick model of the deck, supported on elastic translational spring elements, representing the abutments and the piers. It is clear, that such an approach simplifies the design procedure, since iterations with respect to the equivalent cantilever heights are no longer required. In Figure 8, the derived target-displacement profile (Δ_i) is compared with the corresponding profile of the previous (general) case, where deck torsional stiffness was set equal to 20% of the uncracked value. Despite the slight discrepancy in column displacements (ascribed to the different participation factors of the first two modes), the simplified design procedure yielded a longitudinal steel ratio of 42.2‰ and 62.3‰ for Col_1 and Col_2, respectively, attributed mainly to the increased required ratios of the secant-to-uncracked column stiffnesses ($K_{eff,i}/K_{g,i}$) (resulting from the significant reduction of $K_{g,i}$). It is seen that despite the fact that a zero torsional stiffness assumption simplifies the design procedure, it also overestimates the required longitudinal steel ratios and leads to uneconomical design.

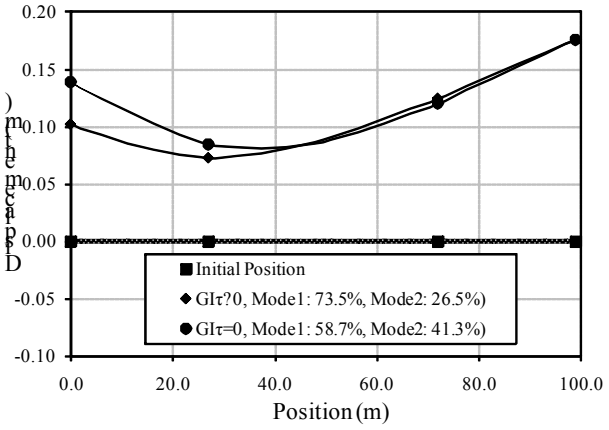

Figure 8. Target-displacement profile (Δ_i) in the case of finite and zero deck's torsional stiffness (GI_τ), (Zone II, D = 1.5 m, in both cases).

5.4 Assessment of MDDBD by NLRHA

The proposed DDBD procedure was assessed using nonlinear response-history analysis (NLRHA) for artificial records closely matching the design spectrum. The artificial records were generated with the computer program SIMQKE [31], while nonlinear analyses were carried out using the SAP2000 software [30]; appropriate nonlinear links were introduced in the finite element model (Figure 3) for response-history analysis, in line with the well-known lumped plasticity approach. The assessment focussed mainly on the target-displacement profiles and on design quantities such as yield displacements, displacement ductilities, stiffnesses, and magnitude of forces developed in critical members of the bridge.

Since the primary objective of the assessment was the study of the transverse bridge response under a seismic excitation which matches as closely as feasible the 'design excitation' (i.e. the design spectrum), one set of NLRHAs was performed for each case (Zone II, III), using artificial records compatible with the design spectra (Figure 4). The set consisted of seven artificial records that fitted the linear design S_a spectra of Figure 4. The Hilber et al. a = -0.1 integration method was selected in SAP2000 [28], which utilises lumped plasticity elements (NLLinks) with rotational spring. Herein, the Takeda degrading-stiffness model [22], also assumed for design (to estimate ξ_i), was adopted. Moment-rotation (M-θ) relationships, assigned to NLLinks used in the finite elements models, were defined from moment-curvature analyses performed for each pier section, utilizing the computer program RCCOLA-90 [32].

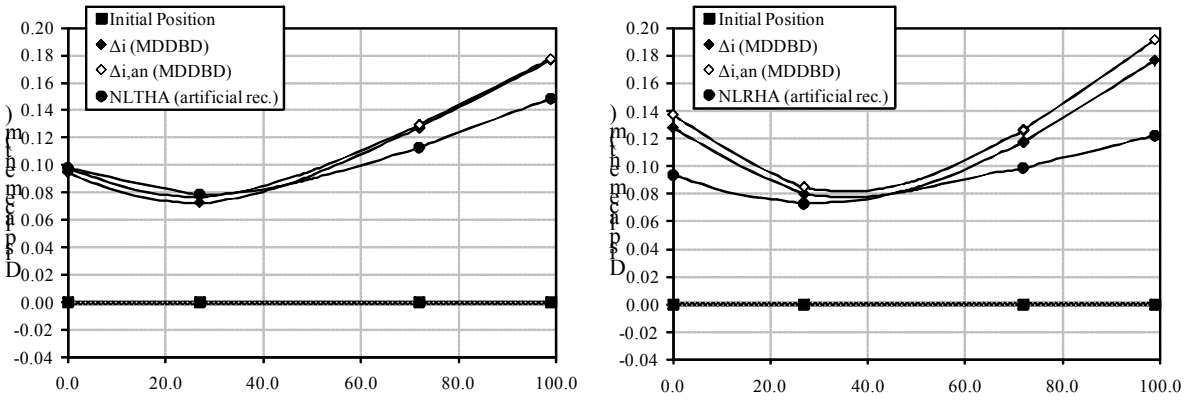

(a) Zone II (PGA=0.24*g*) (b) Zone III (PGA=0.36*g*)

Figure 9: Nonlinear response history maximum displacements: (a) Zone II (PGA=0.24*g*), (b) Zone III (PGA=0.36*g*), compared with target-displacements profiles (Δ_i) and displacement profiles obtained from structural analyses (Δ_{ani}) of Modal DDBD.

In Figure 9 the target-displacement profiles and the displacement profiles obtained from structural analyses within the MDDBD procedure are compared with the displacement envelopes from NLRHA; it is noted that the deck displacements shown in the figures as the NLRHA case are the average of the maximum displacements recorded in the structure during the seven RHAs of each set. It is observed that the target-displacement profiles derived from MDDBD tend to match that obtained from NLRHA, more so in the case of Zone II. The main difference between MDDBD and NLRHA is noted towards the abutments of the bridge (critical members of design), with differences diminishing in the area of the piers. These differences may be attributed to a higher mode contribution (modes not taken into account in the MDDBD) and/or to the contribution of the first two modes with different participation factors than those obtained from the EMS method. However, the displacement demand in the critical member (the one that governs the design – herein Abutment 2) obtained from NLRHA, never

exceeds the design displacement, indicating a safe design. A minor exceedance was only observed in the case of Col_1 (see also Figure 10).

Similar conclusions are drawn with respect to the other design quantities; yield displacements, displacement ductilities, bearing shear strain and column drift ratios obtained from NLRHAs were compared with those estimated at the design stage. Figure 10 (supplemented by Table 2) illustrates the correlation in the above quantities, in the case of Zone II. Again, curves shown in the figures as the NLRHA case are the average of the quantities recorded in the structure during the seven RHAs (either at the time step each member enters the inelastic range or at the time step of maximum response), whereas curves shown as MDDBD were computed from the results of structural analyses. It is clear that MDDBD predicts very well, (i.e. matches closely the values from the NLRHA approach), the quantities related to member yielding, which implies the effectiveness of the equivalent cantilever approach in capturing the degree of fixity at the top of the piers, despite the fact that during the design procedure the equivalent cantilever heights are computed according to moment diagrams at maximum response (and not the response at the time of yielding). Finally, difference in member shear force at maximum response is mainly attributed to the consideration of strain hardening in M-θ relationships used in the assessment, whereas MDDBD assumes zero post-elastic slope of the member force-displacement response. In conclusion, the overall agreement between MDDBD and NLRHA is deemed satisfactory.

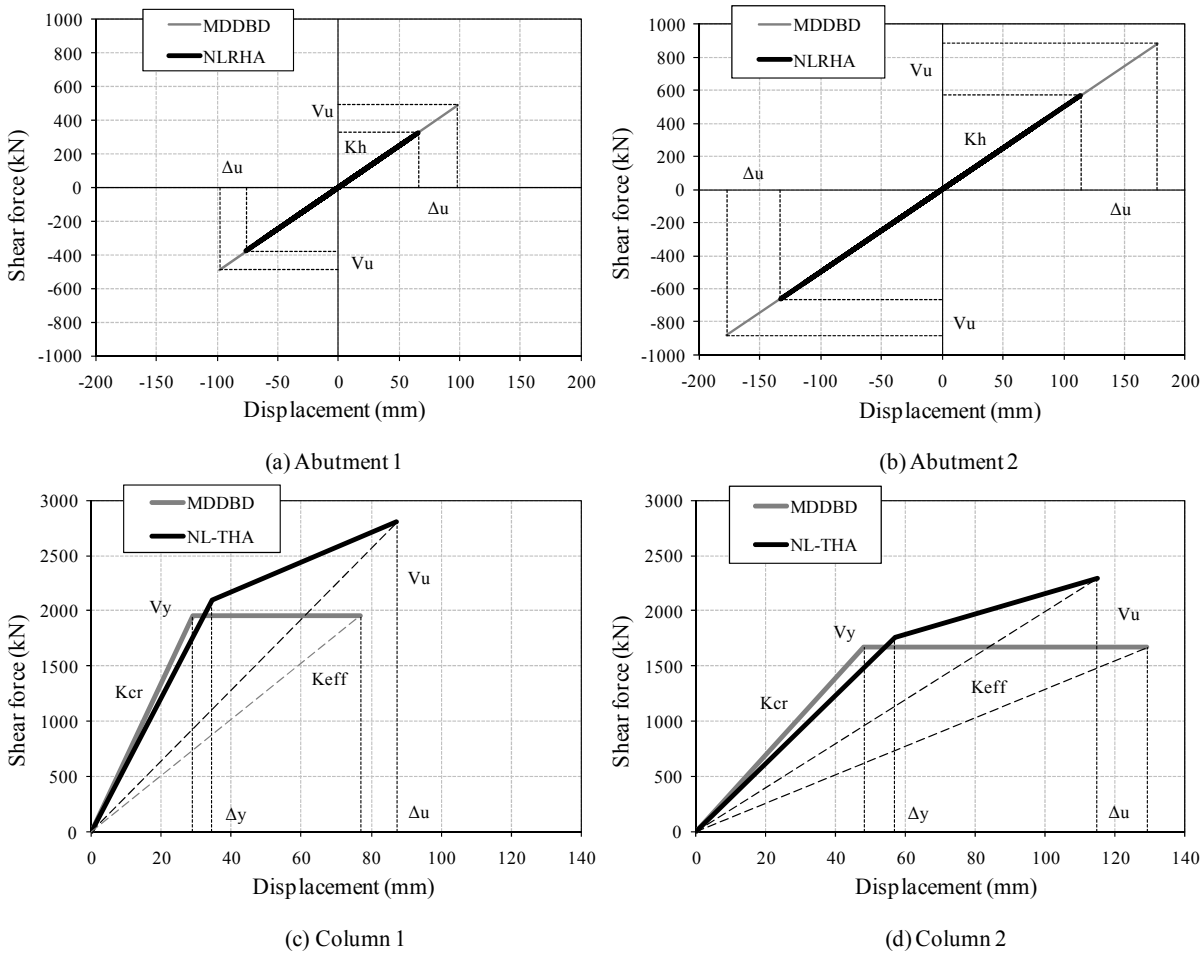

Figure 10: Member shear force-displacement curves derived from modal direct displacement-based design (MDDBD) and nonlinear response history analyses (NLRHA) in the case of artificial records and Zone II (PGA=0.24*g*).

Member	Abutment 1		Abutment 2		Column 1		Column 2	
	MDDBD	NLRHA	MDDBD	NLRHA	MDDBD	NLRHA	MDDBD	NLRHA
Δ_y (mm)					29	35	48	57
V_y (kN)					1958.6	2102.3	1668.5	1757.1
Δ_u (mm)	98	76	177	133	77	87	129	115
V_u (kN)	489.5	378.8	882.6	663.7	1958.6	2804.3	1668.5	2291.2
K_h (kN/m)	5011.4	4980.8	5011.4	4986.9				
K_{cr} (kN/m)					67537.6	60839.1	34760.4	30929.6
K_{eff} (kN/m)					25436.2	32119.7	12934.1	19981.0
μ_Δ					2.66	2.53	2.69	2.02
γ% (γ_u=2.0)	1.11	0.86	2.01	1.51				
Col. Drift (%)					1.06	0.92	1.06	1.21

Table 2. Design quantities in the case depicted in Figure 10.

6 CONCLUSIONS

An existing displacement-based methodology (DDBD) was extended here to account for higher mode effects in the case of bridges. Its feasibility and accuracy were evaluated by applying it to an actual bridge wherein the first two modes dominate the transverse response. The key issue in this extension was the proper definition of N+1 target-displacement profiles and equal in number equivalent SDOF structures for performing the EMS and estimating the peak 'modal' earthquake forces; the peak 'modal' response was then obtained by conducing N structural analyses, (as many as the significant modes), on the MDOF. Additional issues addressed included the columns' degree of fixity, introducing the concept of the equivalent cantilever heights, and the base shear distribution according to the results of structural analysis. The significance of a rational consideration of the superstructure torsional stiffness throughout the design procedure was also underlined.

By applying DDBD and MDDBD, as well as NLRHA, to the aforementioned bridge, it was concluded that:

- The DDBD method failed to reproduce, through the structural analysis, the target-displacement profile (Δ_i), which was anticipated given the fact that the latter represents a fictitious profile consisting from non-synchronous displacements, and eventually reflects the peak (and non-synchronous) structural member response. On the contrary, MDDBD is intrinsically capable of meeting this goal, by producing the target-displacement-profile (Δ_i) and hence the peak structural response.
- The MDDBD provided also a good estimate of results regarding not only the displacement profile but also additional design quantities such as yield displacements, displacement ductilities, values of stiffness and magnitude of member forces, closely matching the results of the more rigorous NLRHA, and indicating at the same time the validity of the equivalent cantilever concept.
- Investigation concerning the effect of the girder's torsional stiffness throughout the suggested methodology revealed the significance of a properly selected value according to the current bridge design philosophy. In contrast, the simplified design procedure, based on the assumption of a simple cantilever column behaviour under lateral earthquake forces, resulted in significantly overestimated longitudinal steel ratios.
- On the basis of the results obtained for the studied bridge, MDDBD can be further simplified, as far as the required iterations in the EMS methodology (Steps 2 to 6) are con-

cerned. Given that whenever the target-displacement profile Δ_i stabilized, the modal target-displacement profiles $U_{i,j}$ also stabilized, Δ_i (and hence the characteristics of the corresponding SDOF) should be used as the sole convergence criterion during Steps 2 to 6. $U_{i,j}$ and hence the remaining SDOFs should be used only in the last iteration (i.e. during the 4th iteration of Figure 7, instead of the 1st, 2nd, 3rd and 4th) in order to define the peak 'modal' earthquake forces (base shears of Equation (18)). This simplification reduces the amount of required calculations.

- More work is clearly required, to further investigate the effectiveness of MDDBD by applying it to bridge structures with higher mode contribution (even more significant that in the bridge studied here), since MDDBD is expected to be even more valuable for the proper estimation of the actual inelastic response and hence for the efficient design of bridges with significant higher modes. Further investigation is also required in the case of different abutment type configuration (i.e. superstructure's transverse displacement restrained at the abutments through seismic links – activation of the abutment-backfill system), where the shear carried by the abutment is not known during the design procedure.
- The MDDBD method proposed herein, as a rule requires a substantial number of iterations; therefore an implementation of the proposed procedure in a software package would significantly increase its usefulness in practical design.

ACKNOWLEDGEMENTS

The contribution of Asst. Prof. A. Sextos and Dr. I. Moschonas (from the Department of Civil Engineering of the Aristotle University of Thessaloniki) to the computational aspects of this work is gratefully acknowledged.

REFERENCES

[1] T.J. Sullivan, G.M. Calvi, M.J.N. Priestley, M.J. Kowalsky, The limitations and performances of different displacement based design methods. *Journal of Earthquake Engineering*, **7**(1), 201–241, 2003.

[2] J.P. Moehle, Displacement based design of RC structures subjected to earthquakes. *Earthquake Spectra*, **8**(3), 403–428, 1992

[3] M.J.N. Priestley, Myths and fallacies in earthquake engineering – Conflicts between design and reality. *Proceedings of the Tom Paulay Symposium – Recent Developments in Lateral Force Transfer in Buildings*, San Diego, 229–252, 1993.

[4] M.J.N. Priestley, Performance based seismic design. *Proceedings of the 12th World Conference on Earthquake Engineering*, Auckland, NZ, Paper No.2831, 2000.

[5] M.J. Kowalsky, M.J.N. Priestley, G.A. MacRae, Displacement-based design of RC bridge columns in seismic regions. *Earthquake Engineering and Structural Dynamics*, **24**(12), 1623–1643, 1995.

[6] M.J. Kowalsky, M.J.N. Priestley, Experimental verification of direct displacement-based design and development of approach for multiple degree of freedom systems. *Proceedings of the National Seismic Conference on Bridges and Highways, Progress in Research and Practice*, Federal Highway Administration, Sacramento, CA, 651–665, 1997.

[7] G.M. Calvi, G.R. Kingsley, Displacement based seismic design of multi-degree-of-freedom bridge structures. *Earthquake Engineering and Structural Dynamics*, **24**, 1247–1266, 1996.

[8] Seismology Committee of Structural Engineers Association of California (SEAOC), *Recommended Lateral Force Requirements and Commentary (Blue Book)*, Sacramento, California, 1999.

[9] M.J. Kowalsky, A displacement-based design approach for the seismic design of continuous concrete bridges. *Earthquake Engineering and Structural Dynamics*, **31**, 719–747, 2002.

[10] H. Dwairi, M. Kowalsky, Implementation of inelastic displacement patterns in direct displacement-based design of continuous bridge structures. *Earthquake Spectra*, **22**(3), 631–662, 2006.

[11] A.J. Kappos, I. Gidaris, K.I. Gkatzogias, "An Improved Displacement-Based Design Procedure for Concrete Bridges", *3rd International Conference on Seismic Retrofitting*, Tabriz, Iran, 20-22 October 2010.

[12] M.J.N. Priestley, G.M. Calvi, M.J. Kowalsky, *Direct displacement-based design of structures*. IUSS Press, Pavia, Italy, 2007.

[13] G. Adhikari, L. Petrini, G.M. Calvi, Application of direct displacement based design to long span bridges. *Bulletin of Earthquake Engineering*, **8**(4), 897–919, 2010

[14] A.K. Chopra, R.K. Goel, A modal pushover analysis procedure for estimating seismic demands for buildings. *Earthquake Engineering and Structural Dynamics*, **31**(3), 561–582, 2002.

[15] T.S. Paraskeva, A.J. Kappos, A.G. Sextos, Extension of modal pushover analysis to seismic assessment of bridges. *Earthquake Engineering and Structural Dynamics*, **35**(11), 1269-1293, 2006.

[16] M.J. Kowalsky, Deformation limit states for circular reinforced concrete bridge columns. *Journal of Structural Engineering*, **126**(8), 869-878, 2000.

[17] C.P. Katsaras, T.B. Panagiotakos, B. Kolias, Effect of torsional stiffness of prestressed concrete box girders and uplift of abutment bearings on seismic performance of bridges. *Bulletin of Earthquake Engineering*, **7**:363–375, 2009.

[18] Ministry of Public Works of Greece, *Guidelines for Earthquake Resistant Design of Bridges (E39)*, Athens, 2007, (in Greek).

[19] M.J.N. Priestley, F. Seible, G.M. Calvi, *Seismic Design and Retrofit of Bridge Structures*. Wiley, New York, 1995.

[20] H.M. Dwairi, *Equivalent Damping in Support of Direct Displacement-Based Design with Applications to Multi-Span Bridges*. Ph.D. dissertation, North Carolina State University, Raleigh, NC, 2004.

[21] C.A. Blandon, M.J.N. Priestley, Equivalent viscous damping equations for direct displacement-based design. *Journal of Earthquake Engineering*, **9**, 257-278, 2005.

[22] C. Guyader, W.D. Iwan, Determining equivalent linear parameters for use in a capacity spectrum method of analysis. *Journal of Structural Engineering*, **132**(1), 59-67, 2006.

[23] H.M. Dwairi, M.J. Kowalsky, J.M. Nau, Equivalent Damping in Support of Direct Displacement-Based Design. *Journal of Earthquake Engineering*, **11**, 512–530, 2007.

[24] T. Takeda, M. Sozen, N. Nielsen, Reinforced concrete response to simulated earthquakes. *Journal of the Structural Division, ASCE*, **96**(12), 2557–2573, 1970.

[25] D.N. Grant, C.A. Blandon, M.J.N. Priestley, *Modeling Inelastic Response in Direct Displacement-Based Design*. Report No. ROSE 2004/02, European School of Advanced Studies in Reduction of Seismic Risk, Pavia, Italy, 2004.

[26] Ministry of Public Works of Greece, *Greek Seismic Code-EAK 2000*, Athens, 2000 (amended June 2003), (in Greek).

[27] CEN (Comité Européen de Normalisation), *Eurocode 8: design of structures for earthquake resistance–Part 2: Bridges*, Brussels, 2005.

[28] M. Fischinger, D. Beg, T. Isakovic, M. Tomazevic, R. Zarnic, Performance based assessment—from general methodologies to specific implementations. *International Workshop on PBSD, Bled, Slovenia*, 293–308, 2004 (published in PEER Report 2004-05 (UC Berkeley)).

[29] K.I. Gkatzogias, *Displacement-based design of RC bridges*. M.Sc. Dissertation, Aristotle University of Thessaloniki, 2009, (in Greek).

[30] Computers and Structures Inc, *SAP2000: Three Dimensional Static and Dynamic Finite Element Analysis and Design of Structures*. Computers and Structures Inc.: Berkeley, CA, 2009.

[31] E.H. Vanmarcke, *SIMQKE*: *A Program for Artiificial Motion Generation*. Civil Engineering Department, Massachusetts Institute of Technology, 1976.

[32] A.J. Kappos, *RCCOLA-90: A Microcomputer Program for the Analysis of the Inelastic Response of Reinforced Concrete Sections*. Imperial College, London, 1996. (Revised at the Department of Civil Engineering, Aristotle University of Thessaloniki, Greece, 2002).